International Journal of High Speed Electronics and Systems
Vol. 13, No. 2 (2003) 575–600

World Scientific
www.worldscientific.com

PLASMA WAVE ELECTRONICS

MICHAEL S. SHUR
Electrical, Computer and Systems Engineering Department
Rensselaer Polytechnic Institute, Troy, NY 12180-3590, USA

VICTOR RYZHII
Computer Solid State Physics Lab, University of Aizu, Aizu-Wakamatsu 965-8580, Japan

Plasma waves are oscillations of electron density in time and space. In deep submicron field effect transistors plasma wave frequencies lie in the terahertz range and can be tuned by applied gate bias. Since the plasma wave frequency is much larger that the inverse electron transit time in the device, it is easier to reach "ballistic" regimes for plasma waves than for electrons moving with drift velocities. In the ballistic regime, no collisions of electrons with impurities or lattice vibrations occur on a time scale on the order of the plasma oscillation period, and the device channel acts as a resonant cavity for the plasma waves, making possible tunable resonant detection or even emission of the electromagnetic radiation in the terahertz range. We review the theory of plasma waves in field effect transistors; discuss instabilities of these waves in different device structures and their applications for detection and generation of the terahertz radiation.

Keywords: Terahertz radiation, plasma waves, ballistic transport, resonant tunneling.

1. Introduction

The terahertz range of frequencies is often referred to as the "terahertz gap", since this frequency range lies in between the frequency ranges of electronic and photonic devices. The upper frequency limit of transistors operating in conventional regimes is limited by the transit time of carriers under the gate (for a field effect transistor) or across the base and collector depletion region (for a bipolar junction transistor). Scaling of feature sizes of silicon Metal Oxide Semiconductor Field Effect Transistors (MOSFETs) and compound semiconductor Heterostructure Field Effect Transistors (HFETs) and Heterojunction Bipolar Transistors has pushed the device parameters into the region, where the transistor operation at a few hundred gigahertz became feasible. [1] However, device feature sizes approach the values, such that fundamental physics limitations lead to diminishing returns on investment in further scaling, and the transit time limited regimes face these limitations in trying to approach the terahertz range of frequencies. On the other hand, since the quanta of terahertz radiation are much smaller than the thermal energy at room or even at liquid nitrogen temperatures, photonic devices using interband or intersubband transitions have to operate at cryogenic temperatures (see Fig. 1).

Plasma waves are oscillations of electron density in time and space, and in deep submicron field effect transistors, typical plasma frequencies, ω_p, lie in the terahertz range and do not involve any quantum transitions. Hence, using plasma wave excitation for detection and/or generation of terahertz oscillations is a very promising approach, and, as illustrated by Fig. 1, the terahertz gap in the electromagnetic spectrum between electronic and photonic devices can be closed by plasma wave electronics devices. We call this approach *plasma wave electronics*. [2-4]

The properties of plasma waves depend on the electron density and on the dimensions and geometry of the electronic system. In a three dimensional case, the

plasma oscillation frequency is nearly independent of the wave length, in a gated two-dimensional electron gas (2DEG), the plasma wave have a linear dispersion law similar to that of sound waves or light in vacuum. In this case, the plasma wave velocity, s, is proportional to the square root of the electron sheet density and can be easily tuned by the gate bias that controls the 2DEG density.

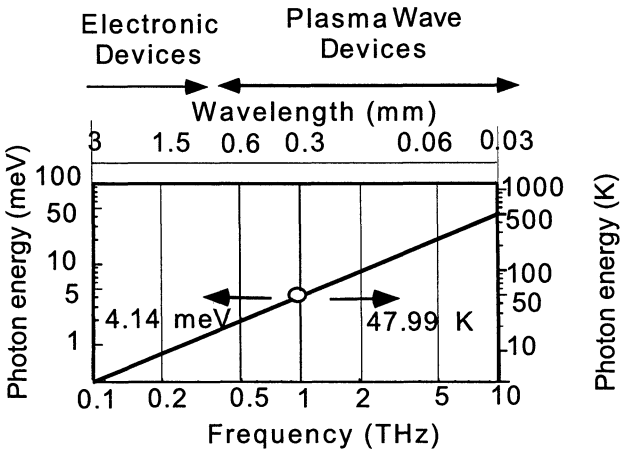

Fig. 1. Terahertz range

This is the physical basis for plasma wave electronics devices that involve two dimensional electrons in a field effect transistor [2-4] or in quantum well structures. [5,6] In deep submicron devices, the electron transit time might become comparable to or even smaller than the electron momentum relaxation time, τ_m. Under such conditions, the electron transport approaches the ballistic regime.[7] (Recently, the Lucent group reported on a ballistic transistor[8], and Kawaura et al demonstrated a 14 nm transistor.[9]) For electrons moving in a device channel with a certain drift velocity, there are two ramifications of the ballistic mode of transport.

In low electric fields, the effective electron mobility in short channel (submicron) devices might be much smaller than the electron mobility in long channel devices. This reduction was predicted for ballistic devices in [10],[11],[12], and, as was shown recently[13], is consistent with experimental data for submicron AlGaAs/GaAs High Electron Mobility Transistors (HEMTs). This ballistic effect should be also important in short channel devices implemented in silicon, silicon-germanium, AlN/GaN/InN or any other semiconductors. The physical reasons for a drastic mobility reduction are related to the ballistic motion first predicted in 1979. [6] In ballistic field effect transistors, electrons travel from the source to the drain without any collisions with impurities or phonons, and electrons propagate in the device channel with a randomly oriented thermal velocity,

$$v_{th} = \left(\frac{8k_B T}{\pi m} \right)^{1/2} \tag{1}$$

(where m is the effective mass, k_B is the Boltzmann constant, and T is temperature) or with a Fermi velocity, v_F, for a degenerate electron gas. Hence, electrons have only a limited time to accelerate in the electric field and acquire a drift velocity. This

acceleration time is determined by L/v_{th}, where L is the device length, (or by L/v_F in a degenerate case). As a result, in low electric fields, the current is proportional to the electric field and to the electron concentration, just like in the collision-dominated case, but the electron mobility has to be substituted by an effective "ballistic" mobility, which (for a non-degenerate case) is given by [11]

$$\mu_{ballistic} = \frac{2qL}{\pi m v_{th}} \tag{2}$$

In high electric fields, electron velocity in a ballistic device is expected to be higher or even much higher that in a collision dominated device [7], and the bulk plasma oscillations should lead to space oscillations of the electron density and resulting S-type current-voltage characteristic. [14]

Plasma oscillations in a field effect transistor are affected by streamlines of the electric field directed from the channel toward the gate, and the velocity of plasma waves in a field effect transistor is typically much higher (by an order of magnitude or more) than the electron drift velocity. Hence, the characteristic transit time is much shorter, and the condition $\omega_p\tau_m > 1$ is much easier to meet that the condition $2\pi\tau_m/t_{tr} > 1$, where t_{tr} is the electron transit time. When the condition $\omega_p\tau_m > 1$ is met, a channel of a field effect transistor can serve a resonant cavity for the plasma waves. As discussed below, the fundamental frequency of this cavity can be tuned by changing the gate bias, and a high mobility deep submicron FET can be used for resonant detection, mixing, multiplication, [15] and even generation [16] of terahertz radiation.

We will start from a general discussion of plasma waves for different geometries with a special emphasis on the plasma waves in a FET channel used for plasma wave electronics. We will then consider the analogy between plasma waves in gated two-dimensional electron gas (2DEG) and shallow water waves and the analogy between plasma waves in ungated 2DEG and deep water waves. This will be followed by the analysis of the instability of plasma waves in gated 2DEG channels. We will then review experimental results on resonant and non-resonant detection and new ideas on using resonant tunneling structures for sharpening surface plasmon resonances.

2. Plasma Wave Oscillations

Following [17], let us consider plasma wave oscillations in the systems of different dimensions by neglecting collisions and considering only the average drift velocity, **v**. The dispersion relations for plasma waves can be derived from the small signal equation of motion and the continuity equation, which, under these assumptions, are given by:

$$\frac{\partial \mathbf{j}}{\partial t} = \mathbf{E}\frac{e^2 n}{m}. \tag{3}$$

$$\frac{\partial \rho}{\partial t} + div\mathbf{j} = 0. \tag{4}$$

where $\mathbf{j} = qn\mathbf{v}$ is the current density, e is the electronic charge, n is the electron density, m is the electronic effective mass, and ρ is a small-signal charge density related to a deviation of n from its equilibrium value, $\mathbf{E}$ is the small signal electric field. Eq. (3) follows from the Newton Second Law of Motion, where electron scattering is neglected. For a 3D geometry, the $\mathbf{j}$, n, and ρ are current per unit area, electron concentration, and

electric charge per unit volume, respectively, whereas in the 2D case, the **j**, n, and ρ are , whereas in the 2D case, the **j**, n, and ρ are current per unit length, electron concentration per unit area, and the electric charge per unit area, respectively.

Differentiating Eq. (4) with respect to time and using Eq. (3), we obtain:

$$\frac{\partial^2 \rho}{\partial t^2} + \frac{q^2 n}{m} div\mathbf{E} = 0 . \tag{5}$$

For the three dimensional case, the relation between **E** and ρ is given by:

$$div\mathbf{E} = \frac{\rho}{\varepsilon} . \tag{6}$$

where ε is the dielectric permittivity. Substituting Eq. (6) into Eq. (5), we obtain the well-known expression for the 3D plasma frequency

$$\omega_p = \sqrt{\frac{q^2 n}{\varepsilon m}} , \tag{7}$$

where ε is the dielectric permittivity of a semiconductor.

For electrons under the gate of an FET, the electron sheet concentration in the channel is proportional to the voltage difference between the gate and channel potentials:

$$qn = CU . \tag{8}$$

Here $U = U_g - U_c - U_T$, U_T is the threshold voltage, $U_g - U_c$ is the potential difference between the gate and the channel, $C = \varepsilon/d$ is the gate-to-channel capacitance per unit area, and d is the gate-to-channel separation. This equation is valid when U changes along the channel on the scale large compared to d (so-called gradual channel approximation). From Eq. (8), we find the relationship between the electric field $\mathbf{E} = -\nabla U$ and two-dimensional charge density $\rho = q(n - n_o)$

$$\mathbf{E} = -\frac{1}{C}\nabla\rho . \tag{9}$$

Substituting Eq. (7) into Eq. (3), we obtain the two-dimensional wave equation for the surface charge ρ

$$\frac{\partial^2 \rho}{\partial t^2} - s^2 \Delta\rho = 0 . \tag{10}$$

where Δ is the two-dimensional Laplace operator, and

$$s = \sqrt{\frac{q^2 nd}{m\varepsilon}} = \sqrt{\frac{qU}{m}} . \tag{11}$$

is the velocity of the surface plasma waves that have a linear dispersion law:

$$\omega_p = sk . \tag{12}$$

Here k is the wave vector of the plasma waves. Using Eq. (6) and (7), we can express the plasma wave velocity in terms of the gate voltage swing:

In a similar way, using Eq. (6) and the relation between the in-plane electric field and surface charge density, one can obtain the dispersion law for the plasma waves for ungated 2D electron gas

$$\omega_p = \sqrt{\frac{q^2 n}{2m\varepsilon}}k \,. \tag{13}$$

and for the plasma waves propagating along a one-dimensional wire:

$$\omega_p = s_1 k\left(\ln\frac{1}{kr}\right)^{1/2} \,. \tag{14}$$

Here r is the radius of the wire, s_1 is the velocity of the one-dimensional plasma waves given by

$$s_1 = \sqrt{\frac{nq^2}{4\pi m\varepsilon}} \,. \tag{15}$$

The case of a gated wire is very similar to that of a FET channel:

$$\omega_p = s_{1d}k \,. \tag{16}$$

where

$$s_{1d} = \sqrt{\frac{q^2 n}{mC_{1d}}} = \sqrt{\frac{qU}{m}} \,, \tag{17}$$

$$C_{1d} = 2\pi\varepsilon\frac{r+d_o}{d_o} \,. \tag{18}$$

The equations for the ungated 2D gas are valid when $kd << 1$ (in the opposite limiting case $kd>>1$ the existence of the metallic gate is irrelevant, and one obtains the dispersion relation given by Eq. (13)). For the 1D case, Eq. (16) holds when $kr << 1$.

Fig. 2 gives the summary of the plasma wave frequencies and dispersion relations for systems of different dimensions and geometry.

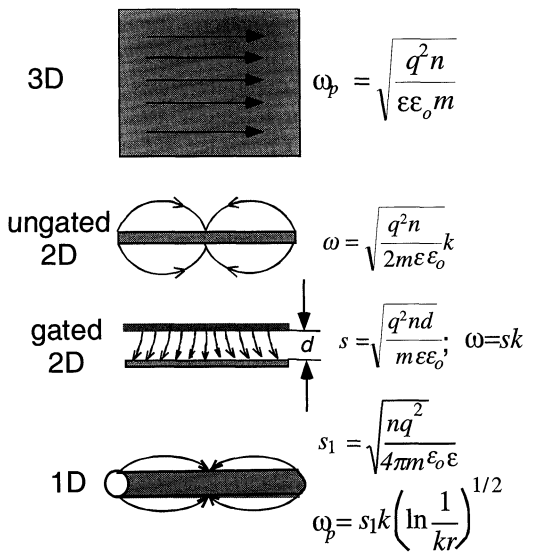

Fig. 2. Plasma wave frequencies for different sample geometries. [3]

Fig. 3 shows the dispersion relations for different geometries. (The dispersion curve calculations for Fig. 3 used the following parameters: dielectric constant, ε_r = 12.9, effective mass, $m_r = 0.067\ m_o$; 3D electron concentration, $n_{3d} = 5\text{x}10^{24}$ m^{-3}, 2D electron concentration, $n_{2d} = 1.5\text{x}10^{12}$ m^{-2}, 1D electron concentration, $n_{1d} = 1.41\text{x}10^{8}$ m^{-1}, gate-to-channel separation for the 1D gated structures, d_o = 3 nm, quantum wire radius, r = 3 nm.)

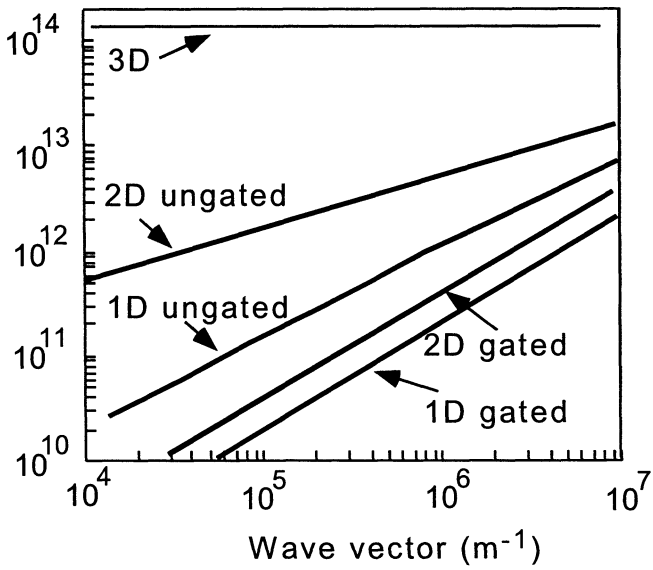

Fig. 3. Plasma wave dispersion relations for different geometries.

The similarity between the dispersion relations for the gated 2DEG case and gated and ungated 1DEG case implies that the results discussed below for the gated 2DEG should equally apply to gated and ungated quantum wires.

In ultra quantum limit in quantizing magnetic fields, it is possible to achieve a situation when electrons propagate as 1D particles but electrostatic interaction is three dimensional. This happens if the electron energy is less than the separation between the Landau subbands and optical phonon energy. In such a system, quasi-elastic collisions of electrons (with impurities and acoustic phonons) can only invert the direction of the electron propagation. This can minimize the effect of these collisions on plasma instabilities. As an example, Ivanov and Ryzhii considered the instability of the electron plasma optically generated in the lowest Landau subband.[18] The dispersion equation for this system coincides with that for two colliding electron beams both in a classical case (for small wave numbers) and in a quantum case (when Wigner equation should be used). It is instructive that elastic scattering does not influence the instability threshold.

The same authors (jointly with Yu. Sigov and V. Kustov modeled the dynamics of this instability (which they called the collective relaxation) using a ensemble particle method and observed fast transformation of the distribution function due to interaction with the self-consistent electric field (unpublished). This instability led to a strong turbulence since its increment was close to the instability frequency.

3. Plasma Waves in FETs

Chaplik [19] was the first to consider plasma waves in a gated 2D electron gas for electrons on the surface of liquid helium. Nakayama. [20] analyzed plasma waves for a FET. Allen et al. [21] observed infrared absorption and Tsui et al [22] observed weak infrared emission related to such waves in silicon inversion layers. More recent studies by Burke et al [23] of high mobility AlGaAs/GaAs gated heterostructures revealed the resonance impedance peaks related to the plasma waves. Dyakonov and Shur used hydrodynamic equations to analyze plasma waves in 2DEG and predicted the instability of plasma waves in a high mobility field effect transistor. [16] They also developed the theory of plasma wave electronics devices, such as detectors and mixers. [15] Lu et al reported the evidence of the resonant plasma wave detection by a FET at the third harmonic. [24] Recently, Knap et al [25] reported on the resonant plasma wave detection by a FET at the fundamental harmonic, and Peralta et al reported on a similar detection in multi gated periodic structures with 2DEG.[26]

The gate electrode in a FET (see Fig. 4) is separated from the channel by the gate insulator (which is a doped or undoped wide band gap semiconductor, such as AlGaAs in a typical High Electron Mobility Transistors and SiO_2 in silicon MOSFETs).

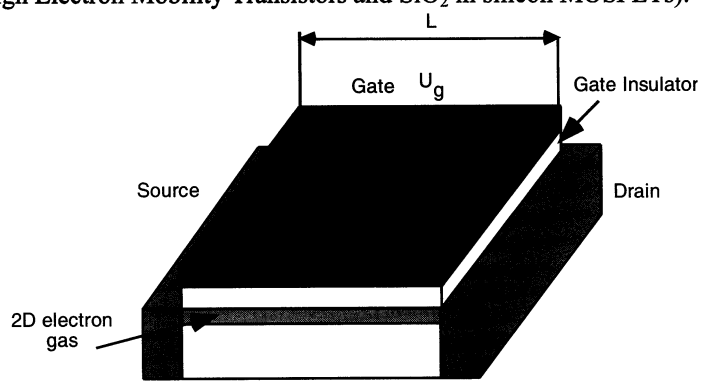

Fig. 4. Field Effect Transistor

A FET operates in two different regimes. At gate biases, V_G, smaller than the FET threshold voltage, V_T, the source and drain contacts are separated by a potential barrier and the current between the source and the drain is very low. An increase in the gate voltage decreases the height of this barrier leading to an exponential rise in current. When $V_G > V_T$, electrons attracted by a more positive gate charge form a narrow sheet of mobile charge at the interface between the semiconductor and the gate insulator. This electron sheet and the gate contact form a capacitor, which capacitance per unit area is where $C = \varepsilon/d$, where d is the gate-to channel separation, Above the threshold, the surface concentration, n_s in the FET channel is given by (see Eq. (8)

$$n_s = CU/q \tag{19}$$

As mentioned above, Eq. (19) represents the usual gradual channel approximation, which is valid when the characteristic scale of the potential variation in the channel is much greater than the gate-to-channel separation, d.

The equation of motion (the Euler equation) is

$$\frac{\partial v}{\partial t}+v\frac{\partial v}{\partial x}+\frac{q}{m}\frac{\partial U}{\partial x}+\frac{v}{\tau_m}=0, \tag{20}$$

where $\partial U/\partial x$ is the longitudinal electric field in the channel, $v(x,t)$ is the local electron velocity, and τ_m is the momentum relaxation time. The usual continuity equation can be written as:

$$\frac{\partial n_s}{\partial t}+\frac{\partial(n_s v)}{\partial x}=0 \tag{21}$$

and re-written as

$$\frac{\partial U}{\partial t}+\frac{\partial(Uv)}{\partial x}=0 \tag{22}$$

taking into account Eq. (19).

In the limiting case of a ballistic FET, τ_m tends to infinity, and Eqs. (20) and (21) coincide with the hydrodynamic equations for shallow water (see, for example, [27]). This means that the 2D-electron fluid in a Ballistic FET should behave like shallow water. In this hydrodynamic analogy, v corresponds to the fluid velocity, and qU/m corresponds to gh, where h is the shallow water level and g is the free fall acceleration.

Hence, phenomena similar to wave and soliton propagation, hydraulic jump, and the "choking" effect [28] should take place in a ballistic hydrodynamic electron fluid. Effects of collisions, surface scattering, changes in the channel cross section, and others may be also understood using this analogy.

In the opposite limited case of a collision dominated transport, Eq. (20) becomes

$$v=-\frac{q\tau_m}{m}\frac{\partial U}{\partial x}=\mu E, \tag{20a}$$

which is usually replaced by a field-dependent velocity function

$$v=v(E), \tag{23}$$

which accounts for the electron velocity saturation in high electric fields and/or for a region of negative differential mobility. Examples of empirical velocity-field dependences are

$$v=\frac{\mu E}{\sqrt{1+(\mu E/v_s)^2}} \tag{24}$$

for electrons in silicon, and

$$v(E)=v_s\left[1+\frac{E/E_s-1}{1+A(E/E_s)^t}\right] \tag{25}$$

for electrons in compound semiconductor materials with a negative differential mobility region, such as GaAs. Here $E_s = v_s/\mu$ is the velocity saturation field, v_s is the electron saturation velocity, and A and t are fitting parameters. The analytical model of a FET, which accounts for the saturation of the electron velocity and for the source and drain series resistances yields the following expressions for the device drain current

$$I_d \approx \frac{g_{ch} U_{ds}}{\left[1+\left(g_{ch} V_{ds} / I_{sat}\right)^m\right]^{1/m}}, \tag{26}$$

where

$$g_{ch} = \frac{g_{cho}}{1+g_{cho}\left(R_s + R_d\right)}, \tag{27}$$

$$g_{cho} == C_i \mu_n \frac{W}{L}\left(U_{gs} - U_T\right) \tag{28}$$

$$I_{sat} = \frac{g_{cho}\left(U_{gs} - U_T\right)}{1+g_{cho}R_s + \sqrt{1+2g_{cho}R_s + \left(\frac{U_{gs}-U_T}{U_L}\right)^2}}, \tag{29}$$

$U_L = E_s L$, and R_s and R_d are source and drain series resistances, respectively.

In the collision dominated regime, operating regime, the upper frequency of operation of a Field Effect Transistor (FET) is limited by the electron transit time, t_{tr}. The transistor cutoff frequency, $f_T = 1/(2\pi t_{tr})$, see for example, [29]. However, plasma effects become important in modern, short channel field effect transistors, where the sheet carrier density is very high. These effects should allow us to use FETs at much higher frequencies (in the terahertz range for deep submicron devices).

A explained above, plasma waves with a linear dispersion law, $\omega = sk$. The velocity of the plasma waves, s, is typically on the order of 10^8 cm/s, which is much larger than the drift velocity of the 2D electrons in the FET channel. This is why the propagation of plasma waves can be used for new regimes of FET operation, with a much higher frequency than for conventional, transit-time limited regimes. Under certain conditions, plasma oscillations can be excited in a FET by a dc current, and the FET can be used as an oscillator operating in the terahertz range. [16] Nonlinear properties of the plasma waves can be utilized for terahertz detectors, broad band detectors, mixers, and frequency multipliers. [30]

Devices operating at terahertz frequencies should be considered to be inseparable from the circuit. Therefore, issues related to coupling plasma wave to electromagnetic radiation conversion, to antenna structures for electromagnetic radiation, and to device integration with submillimeter circuits will have to be addressed for practical implementation of plasma wave electronic devices. Since the plasma wave velocity is much smaller than the light velocity, and the device dimensions are much smaller than the electromagnetic wave length corresponding to the plasma frequency, antenna structures -- which are much larger than typical devices -- are needed for coupling plasma and electromagnetic waves. These issues and the antenna and circuit design will be similar to those currently investigated for deep submicron Schottky diodes operating in the terahertz range. [31]

4. Plasma wave instability

Dyakonov and Shur showed that the surface plasma waves propagating in gated 2DEG) might grow in a ballistic device due to reflections from the device boundaries. [16]

The linearized system of Eqs. (20) (in the limit of $\tau \to \infty$) and (22) predicts the dispersion law, $k = \pm\omega/s$, which is the same as for the shallow water waves. The wave velocity $s = (qU_o/m)^{1/2}$. * If the electrons move with a drift velocity v_o, the waves are carried along by the flow, and the dispersion relation becomes $k = \omega/(v_o \pm s)$. (The drift velocity, v_o, corresponds to the current per unit width $j = qn_sv_o = CU_ov_o/q$.)

Dyakonov and Shur assumed the following boundary conditions at the source and drain side the device channel: constant gate-to-source voltage, U_{gs}, at the source side of the channel ($x = 0$) and constant drain current at the drain side of the channel ($x = L$). The realization of these boundary conditions is straightforward at low frequencies, i.e. one applies voltage between the gate and source using a voltage source, U_{gs}, and connects a current source, I_{ds}, to the drain. At high frequencies, the boundary conditions, such as short and open circuits, cannot be easily implemented. Also, the displacement current between the gate and the channel plays an important a role. However, all microwave, millimeter, and submillimeter field effect transistors designed in such a way that the gate-to-source parasitic and fringing capacitances (which add to the input capacitance) is greater or even much greater than the gate-to-drain parasitic and fringing capacitances (which contribute to the Miller capacitance). The intrinsic gate-to-source and gate-to-drain capacitances are equal at zero drain bias. However, the intrinsic gate-to-source capacitance increases with an increase in the drain bias and the intrinsic gate-to-drain capacitance decreases with an increase in the drain bias (see Fig. 5). †

Therefore, the boundary conditions at the source are closer to the short circuit conditions at high frequencies and the boundary conditions at the drain are closer to the open circuit. This asymmetry increases with an increase in the drain bias as shown in Fig. 5. We let $v = v_o + v_1\exp(-i\omega t)$, $U = U_o + U_1\exp(-i\omega t)$, linearize Eqs. (20), (22) with respect to v_1 and U_1, and use the boundary conditions $U_1(0) = 0$ and $\Delta j(L) = 0$ (i. e., $U_0v_1(L) + v_0U_1(L) = 0$) as discussed above. We then seek the solution as the sum of two waves propagating from the source to the drain and from the drain to the source, respectfully, with the wave vectors k_1 and k_2:

$$v_1 = A\exp(ik_1x) + B\exp(ik_2x) \tag{30}$$

$$U_1 = C\exp(ik_1x) + D\exp(ik_2x) \tag{31}$$

where

---

* The analogy between plasma waves in a FET and water waves goes even further. While for $kd << 1$ the plasma waves with $\omega \sim k$ are similar to the shallow water waves, in the opposite limiting case $kd >> 1$, the plasma waves have the same dispersion law $\omega \sim k^{1/2}$ as the gravitational waves in deep water.

† We should notice that capacitances shown in Fig. 5 are calculated assuming the collision dominated transport in a FET. However, the qualitative conclusions should apply to the ballistic regime as well.

$$k_1 = \frac{\omega}{s_1} = \frac{\omega}{s + v_o} \tag{32}$$

$$k_2 = \frac{\omega}{s_2} = \frac{\omega}{s - v_o} \tag{33}$$

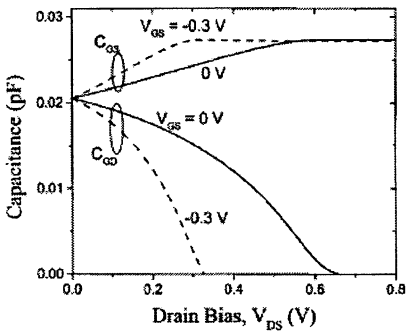

Fig. 5. Gate-to-source and gate-to-drain capacitances for zero and -0.3 gate biases: C_{GS} and C_{GD},versus drain bias. Parameters used in the calculation: threshold voltage, U_T =- 0.6 V; gate width and length W=50 mm and L=0.15 mm, respectively; AlGaAs thickness, d_i = 25 nm; and maximum density of the two-dimensional electron gas, n_{smax} =2.5x10^{16} m^{-2}. [32]

This procedure leads to the following expressions for the real and imaginary parts of $\omega = \omega' + i\omega''$:

$$\omega' = \frac{\left|s^2 - v_o^2\right|}{2Ls}\pi n \tag{34}$$

$$\omega'' = \frac{\left|s^2 - v_o^2\right|}{2Ls}\ln\left|\frac{s + v_o}{s - v_o}\right| \tag{35}$$

where n is an odd integer for $|v_o| < s$ and an even integer for $|v_o| > s$. Eq. (35) shows that for positive v_o, the steady flow is unstable if $v_o < s$ and stable if $v_o > s$. For $v_o/s << 1$, $\omega'' = v_o/L$ which is the inverse electron transit time.

The boundary conditions play a very important role in determining the growth of this plasma instability. Different boundary conditions might be interpreted in terms of effective impedances connected between the source and gate and the gate and drain, respectively (see Fig. 6):

$$Z_{gs} = \frac{U_1(0)}{j_1(0)W} \tag{36}$$

$$Z_{gd} = \frac{U_1(L)}{j_1(L)W} \tag{37}$$

where $j_1 = qn_{s1}v_o + qn_{so}v_1$ and W is the gate width.

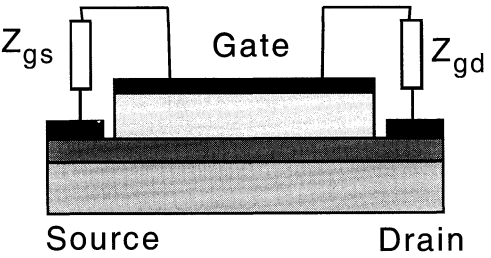

Fig.6. Boundary conditions for plasma waves in FET channel.

Our analysis showed that the instability might take place as long as $|Z_{gs}| << |Z_{gd}|$. A more detailed analysis of different boundary conditions for this system was given by Crowne. [33]

The above analysis is based on the solution of hydrodynamic equations, which are valid when electron-electron collisions are very frequent. Dmitriev et al [34] presented the solution of the Boltzmann equation for a relatively low density gated two-dimensional electron gas, where electron-electron collisions are not significant. This solution revealed that the plasma waves have the same dispersion law as for a high electron sheet density. In both cases, the plasma waves become instable in a short channel field effect transistor with asymmetric boundary conditions at small channel currents. They also investigated the role of the Landau damping. The Landau damping is the damping of a plasma wave caused by a transfer of energy from the wave to particles, whose velocity equals the phase velocity of the wave. In this system, the electron velocity is v_F (or vth in a non-degenerate case) and the plasma wave velocity is s. Dmitriev et al showed that the Landau damping is small when s >> v_F, which is quite understandable. The inequality $s >> v_F$ can be presented as

$$d >> r_s/2 \tag{38}$$

where $r_s = \dfrac{4\pi\varepsilon\hbar^2}{mq^2}$ is the Bohr radius. For GaAs, $\varepsilon = 1.14\text{x}10^{-10}$ F/m, $m = 0.067\ m_o$, where m_o is the free electron mass, and r_s = 10 nm. Typical values of d are on the order of 30 nm, so that Eq. (38) is valid, even though this estimate shows that the Landau damping might be important in devices with a smaller separation between the gate and the channel.

5. Instability conditions

Three decay mechanisms oppose plasma wave growth caused by the instability described in Section 4: electron scattering by phonons or impurities, the effect of the finite electron transit time in the channel leading to the "ballistic mobility" given by Eq. (2), and internal friction caused by the viscosity of the electron fluid.

The electron scattering can be accounted for by retaining the term $-\nu/\tau_m$ in the right-hand side of Eq. (20). This leads to the addition of the $-\ 1/(2\tau_m)$ term to the wave

increment. Hence, the wave grows only if the number of scattering events during the transit time is small.

The viscosity, ν, of the electron fluid causes an additional damping with the decrement of νk^2 where k is the wave vector. Hence, the viscosity is especially effective in damping higher order modes. Comparing ω'' with νk^2 for the first mode, we find that the effect of the viscosity is small when the Reynolds number $\mathrm{Re} = L\, v_o / \nu$ is much greater than unity. In a highly non-ideal electron gas, where the Bohr energy, thermal energy, and Fermi energy are of the same order (which roughly corresponds to the surface electron concentration of 10^{12} cm^{-2} at 77 K in GaAs), the viscosity of the electron fluid is on the order of $\hbar / m$, which is approximately 15 cm^2/s (comparable to that of castor oil or glycerin at room temperature). The Reynolds number may be estimated as $\mathrm{Re} = m v_o L / \hbar \sim 12$ for $v_o = 10^7$ cm/s and $L = 0.2$ μm (see Fig. 7).

For a sample with $L = 0.2$ μm at 77 K, assuming $\tau_m \sim 10^{-11}$ s, the increment v_o/L exceeds the decrement $1/(2\tau_m)$ caused by the collisions when $v_o > 10^6$ cm/s. For the same sample, the decrement caused by viscosity, $\nu(2\pi/L)^2/16$, is smaller then the increment v_o/L when $\nu = \pi^2 \nu / (4L) \sim 1.8\text{x}10^6$ cm/s. Hence, the threshold velocity for the instability is well below the peak velocity in GaAs (~2x10^7 cm/s).

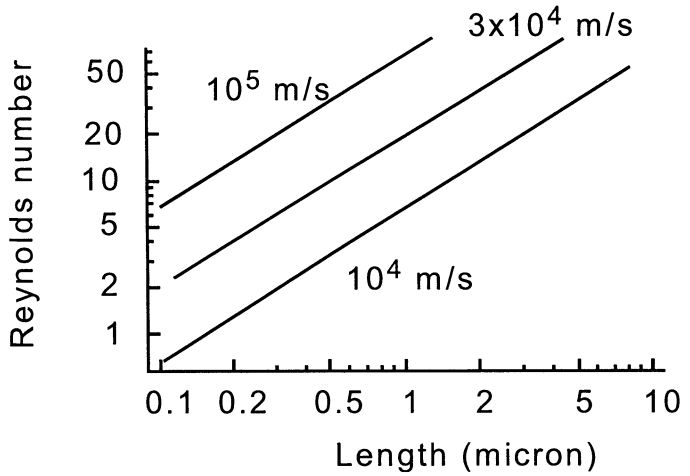

Fig. 7. Reynolds number versus gate length for different velocity values in FET channel

The condition $v_o/L < 1/(2\tau_m)$ corresponds to the requirement of a ballistic transport in a transistor channel. In this regime,

$$v_o = \mu_{bal} U_{ds} / L \tag{39}$$

where U_{ds} is the intrinsic drain-to-source voltage drop across the channel (excluding the voltage drop across the source and drain series resistances) and μ_{bal} is given by Eq. (2) for a non-degenerate case. Hence, the inequality $v_o/L < 1/(2\tau_m)$ can be re-written as

$$U_{ds} > U_{cr} = \frac{1.25L\left(\frac{k_B T}{m_e}\right)^{1/2}}{\mu} \tag{40}$$

Fig. 8 shows the values of U_{cr} and $\nu_{ocr} = L/(2\tau_m)$ for GaAs-based HEMTs versus the gate length at 300 K and 77 K. As seen from these figures, the instability condition can be achieved in deep submicron (less than 0.1 micron or so) devices at room temperature and in one to two micron size (or shorter) devices at 77 K.

The first measurement results by Cheremisin point out that such instability might indeed occur in 0.1 micron CaAs-based HEMTs. [35] However, more experimental studies are needed to prove the existence of this instability.

Recently Ryzhii and Shur [36] proposed to combine this approach with using resonant tunneling structure inserted between the gate and a channel of HEMT or a related NERFET-type device [37] (see Fig. 9). Their theory predicts a very large increase of the plasma wave instability increment. Ryzhii et al.[5] also proposed to use a similar structure to enhance the plasma wave detector sensitivity (see Section 6).

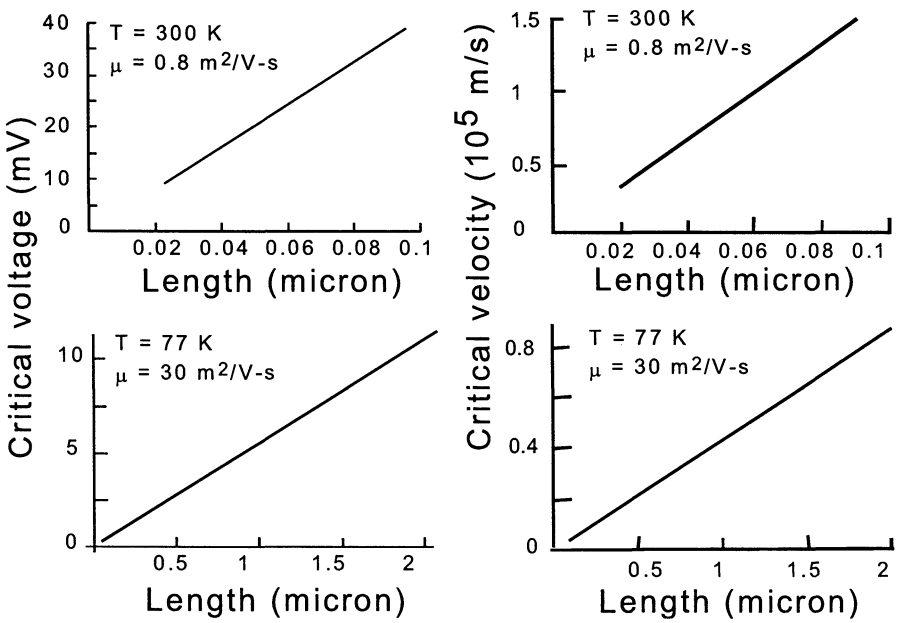

Fig. 8. U_{cr} and $\nu_{ocr} = L/(2\tau_p)$ for GaAs-based HEMTs versus the gate length at 300 K and 77 K

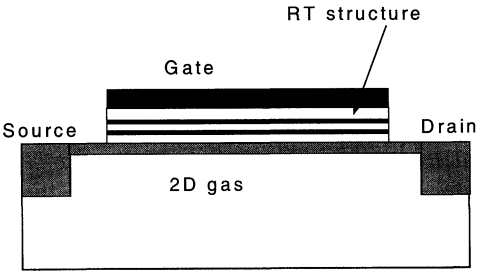

Fig. 9. Resonant tunneling structures for enhancement of plasma wave instability.

For a FET with a resonant tunneling structure between the gate and the channel, Eq. (21) should be re-written as

$$\frac{\partial n_s}{\partial t} + \frac{\partial (n_s \mathrm{v})}{\partial x} = -\frac{n_s}{\tau_e} \Lambda\left(\frac{\varepsilon_{RT}}{\Gamma}\right) \tag{41}$$

where τ_e^{-1} is the product of the try-to-escape frequency and the maximum transmission, $\Lambda(z) = \dfrac{1}{1+z^2}$ is the resonance tunneling form-factor [38], $\varepsilon_{RT} = E_{RT} - qaU/2$ and Γ are the energy and position of the resonant tunneling level, and $a \sim 1$ is a geometrical factor. The boundary conditions for this structure were chosen as

$$U(0) = U(L) = 0 \tag{42}$$

As was shown in Reference [33], the plasma wave frequencies in such system are given by

$$\omega_n \sim s k_n \tag{43}$$

where $k_n = \pi n/L$, and $n = 1, 2, 3 \ldots$

Fig. 10 shows the increment of the instability calculated in Reference [33] for 0.5 micron gate devices. As seen, this instability should take place in submicron GaAs-based HEMTs with a resonant tunneling structure at 77 K, when the electron mobility is large enough.

Ryzhii and Shur also suggested that a forward gate current in FETs can enhance the plasma instability increment. [39] Electrons constituting this current experience the time delay that typically might be on the order of d/v_{eff}, where v_{eff} is the velocity of the electrons crossing from the channel into the gate. Such delay might lead to a dynamic negative conductance at plasma frequencies, which should result in the excitation of plasma waves in the transistor channel.

Once the electron velocity exceeds the threshold, the plasma waves grow. Since no other steady states exist for $v_o < s$, [‡] this growth should lead to oscillations for which the plasma wave amplitude is limited by non-linearity. Nonlinear plasma oscillations in FETs have been studied in References[40,41,33].

Let us now discuss possible applications of this instability. The plasma oscillations result in a periodic variation of the channel charge and the mirror image charge in the

[‡] We should notice that for $|v_o| > s$, in addition to the uniform flow, there is another steady state solution corresponding to a hydraulic jump in shallow water. [16]

gate contact, i. e. to the periodic variation of the dipole moment. This variation should lead to electromagnetic radiation. The device length is much smaller than the wavelength of the electromagnetic radiation, λ_R, at the plasma wave frequency. (The transverse dimension, W, may be made comparable to λ_R). Hence, the Ballistic FET operates as a point or linear source of electromagnetic radiation. Many such devices can be placed into a quasi-optical array for power combining. This device de-couples the operating frequency (which can be tuned in a wide frequency range by varying U_o) from the electron transit time limitation. The maximum modulation frequency is still limited by the transit time.

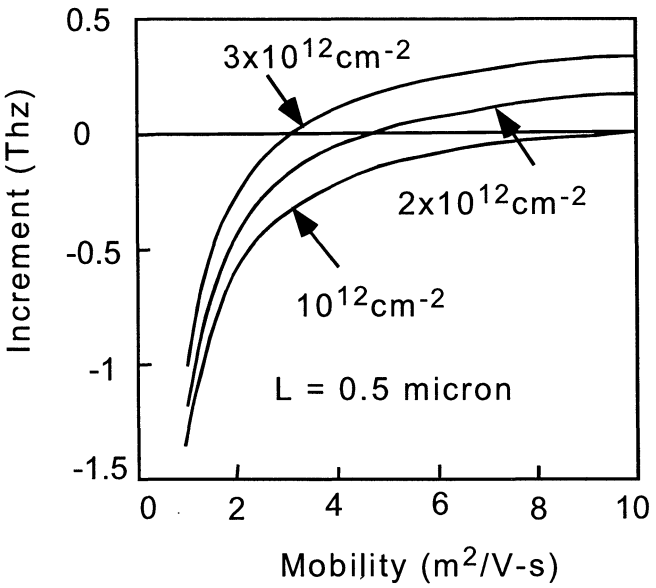

Fig. 10. Increment of fundamental mode versus channel mobility for resonant tunneling HETM structures. [33]

6. Detectors and mixers of terahertz radiation

The excitation of surface plasma waves can be also used for detection, multiplication, and mixing of terahertz radiation. [15] Weikle et al. [42] and Lu et al. [43] reported on the detection of the microwave and terahertz radiations, respectively, using AlGaAs/GaAs HEMTs Fig. 11 shows a schematic diagram and an equivalent circuit of a HEMT subjected to terahertz radiation.

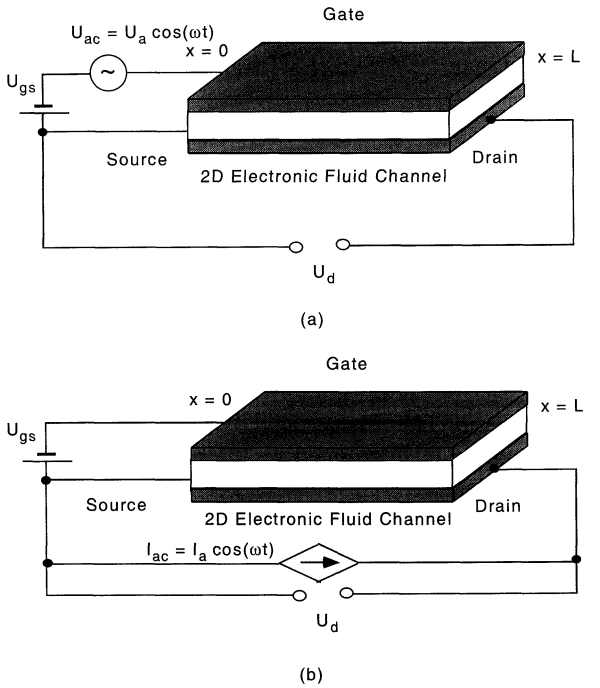

Fig. 11. Schematic geometry of FET operating in detector mode for induced ac voltage (a) and induced ac current (b). [15] © IEEE, 1998

The incoming electromagnetic radiation induces an ac voltage at the source side of the channel. The drain side of the channel is an open circuit. (A coupling with a terahertz radiation might be enhanced using an appropriate antenna structure.) This ac voltage excites the plasma waves. As mentioned above, the dc gate-to-source voltage determines the velocity, *s*, of these waves. Because of the nonlinear properties of the electron fluid and the asymmetry in the boundary conditions, a FET biased only by the gate-to-source voltage and subjected to electromagnetic radiation develops a constant drain-to-source voltage, which has a resonant dependence on the radiation frequency with maxima at the plasma oscillation frequency and its odd harmonics. The induced drain voltage, ΔU, is given by [15]

$$\frac{\Delta U}{U_o} = \frac{1}{4}\left(\frac{U_a}{U_o}\right)^2 f(\omega) \tag{44}$$

where

$$f(\omega) = 1 + \beta - \frac{1 + \beta\cos(2k_o' L)}{\sinh^2(k_o'' L) + \cos^2(k_o' L)} \tag{45}$$

Here

$$\beta = \frac{2\omega\tau}{\sqrt{1+(\omega\tau)^2}}, \tag{46}$$

and $k_o^{'}$ and $k_o^{''}$ are the real and imaginary parts of the wave vector, k_o:

$$k_o^{'} = \frac{\omega}{s}\left(\frac{(1+\omega^{-2}\tau^{-2})^{1/2}+1}{2}\right)^{1/2}, \tag{47}$$

$$k_o^{''} = \frac{\omega}{s}\left(\frac{(1+\omega^{-2}\tau^{-2})^{1/2}-1}{2}\right)^{1/2}, \tag{48}$$

Here where n = 1, 3, 5, 7..., U_o is the gate-to-source gate voltage swing, and U_a is the amplitude of the ac source-to-gate voltage induced by the incoming radiation. The half width of the resonance curve is determined by the damping of the plasma oscillations caused by the electron momentum relaxation and/or the electron fluid viscosity. Thus, the FET acts as a tunable resonance quadratic detector of electromagnetic radiation.

Lu et al reported on the implementation of a terahertz detector utilizing 2D electronic fluid in a High Electron Mobility Transistor (HEMT). [24] To our knowledge, this is the first plasma wave terahertz detector ever demonstrated. The detector was fabricated using a *Fujitsu* FHR20X HEMT mounted on a quartz substrate. The device operated at a frequency of 2.5 THz, which is about 30 times higher than the transistor cutoff frequency. A CO_2-pumped far-infrared gas laser served as a source of terahertz radiation. The laser beam was chopped and focused on the sample with the electric field polarization oriented in the drain-to-source direction. The drain was open, thus the drain current is zero. The gate current is in the order of nano-ampere for the measurement range of gate bias. In agreement with the predictions of our terahertz detector theory [15], the radiation induced a negative DC drain-to-source bias proportional to the radiation intensity. This voltage was measured using a lock-in amplifier. The measured dependencies of the detector responsivity on the gate bias are in good agreement with the gate bias dependence of the normalized responsivity predicted by the detector theory [15] (see Fig. 12). The responsivity increases at smaller gate voltage swings as predicted by the theory. The dimensionless responsivity function displays a rather broad resonant peak corresponding to the third harmonic of the surface plasma frequency.

More recently, Knap et al [44] demonstrated the resonant detection of sub-terahertz radiation by the two-dimensional electron plasma confined in a submicron gate GaAs/AlGaAs field-effect transistors. Their results confirmed that the critical parameter governing the sensitivity of the resonant detection is $\omega\tau_m$, where ω is the radiation frequency and τ_m is the momentum scattering time. By lowering the temperature and hence increasing τ_m and increasing the detection frequency ω, they reached the $\omega\tau_m \sim 1$ condition and observed a resonant detection of 600 GHz radiation in the 0.15 μm gate length GaAs field-effect transistor (see Fig. 13). The evolution of the observed photoresponse signal with temperature and frequency is well reproduced within the framework of a theoretical model developed earlier.

Let us now consider an HFET detector with a longer channel, such that $s\tau_m/L << 1$. In this case, the plasma waves are excited by the incoming radiation near the source, provided that $\omega\tau >> 1$ but they decay before ever reaching the drain side of the channel.

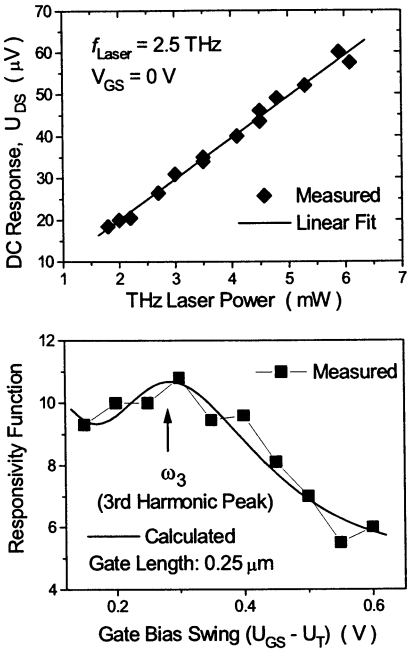

Fig. 12. Measured (symbols) response versus incident power at zero gate bias at 2.5 THz and the laser power of 5.7 mW. The solid line is normalized for comparison. The peak corresponds to the third harmonic of the surface plasma frequency, ω_3.[32] © IEEE, 1998

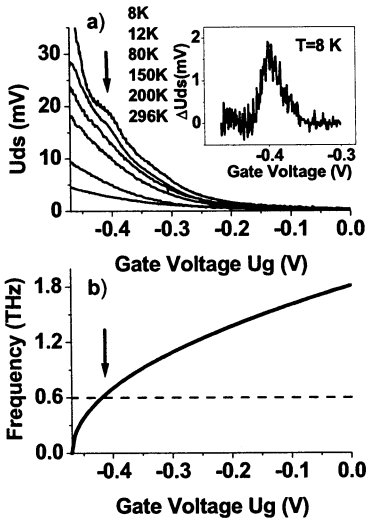

Fig.13 a) Experimental drain response, U_{ds}, for different temperatures. Inset shows the resonant signal ΔU_{ds} at 8 K obtained after subtraction of the $1/U_0$ like background. b) Resonant plasma frequency as a function of the gate voltage. The vertical arrow shows the cross point with 600GHz horizontal line – the voltage of the expected resonant detection. [44]

The analysis of this case, based on the solution of Eqs. (44) - (48), shows that the dc voltage will still be developed between the drain and source, and the device will operate as a broad band detector of electromagnetic radiation with the output signal

$$\frac{\Delta U}{U_o} = \frac{1}{4}\left(\frac{U_a}{U_o}\right)^2 \left(1 + \frac{2\omega\tau_m}{\sqrt{1+\omega^2\tau_m^2}}\right) \tag{49}$$

As can be seen from Eq. (49), a long HFET should act as a broad band detector of electromagnetic radiation. The highest frequency of detection is on the order of s/d where d is the gate-to-source spacing, since the gradual channel approximation is not valid for the plasma wavelengths shorter than d. For $s \sim 10^8$ cm/s and $d \sim 100$ Å, this corresponds to 100 THz.

Weikle et al fabricated a prototype non-resonant detector (operating in the microwave range) using an AlGaAs/GaAs 0.15 micron gate HEMT. [42] The measured dependencies of the detector responsivity on the gate bias and frequency were in good agreement with our theory. AlGaN/GaN HFETs exhibited a non-resonant detection at frequencies much higher than the HEMT cutoff frequency. The measured detector responsivity was in good agreement with the theory and reaches 300 V/W, which is comparable to the responsivity of Schottky diode detectors at these frequencies. This value can be greatly improved by using a proper antenna structure.

More recently, Knap et al [45] reported on an experimental and theoretical study of nonresonant detection of sub-terahertz radiation in GaAs/AlGaAs and GaN/AlGaN heterostructure field effect transistors (see Fig. 14). The experiments were performed in a wide range of temperatures (8-300K) and for frequencies ranging from 100GHz to 600GHz. The photoresponse measured as a function of the gate voltage exhibited a maximum near the threshold voltage. The results were interpreted using a new theoretical model that shows that the maximum in photoresponse and showed explained by the combined effect of exponential decrease of the electron density and the gate leakage current.

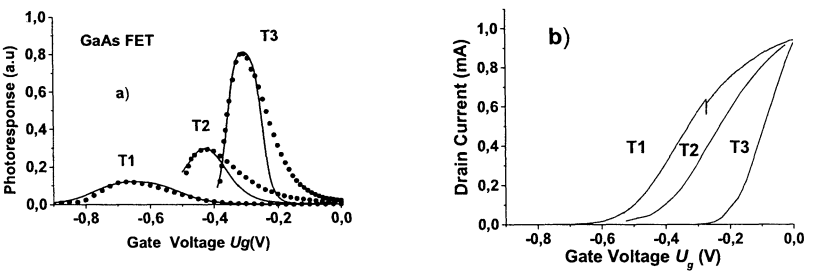

Fig.14. Response at 600 GHz, measured dots, calculated solid lines (a) and drain current versus gate voltage U_g (b) measured in three experiments T1, T2, T3. Results marked as T1 corresponds to the transistor with the threshold voltage U_{th}=~0.55V measured at 300K. Results marked as T2 corresponds to the transistor with U_{th} =-0.42V. Results marked as T3 correspond to the same device but measured at temperature of 10 K, for which the threshold voltage was lower (U_{th} =-0.22V). [45]

These detectors operated at frequencies well above the cutoff frequency. Knap et al obtained similar experimental results for the broadband sub-terahertz detectors fabricated using AlGaN/GaN HFETs. Their results showed that the 2D electron plasma effects are indeed universal, not dependent upon a particular material system (see also [46])

7. Terahertz photomixing using resonant excitation of plasma oscillations

Alternative approaches to generate THz radiation are associated with optical techniques, that use a coherent output at the difference frequency (equal to the difference between the frequencies of radiation emitted by two lasers) or a response of photoconductive structures to femtosecond optical pulses.[47-51] Fast quantum well infrared photodetectors (QWIPs) utilizing intersubband transitions [52] can also be used for the generation of THz radiation by mixing infrared laser beams. Indeed, as shown theoretically, QWIPs can exhibit a marked response to infrared signals in the THz range of modulation frequencies if the electron transit time is short enough (as can be in single QWIPs [53,54]) or if electrons reveal a pronounced velocity overshoot after their photoexcitation from QWs. [55,56] The THz signals produced by coherent plasma oscillations of the photogenerated carriers have been observed in *p-i-n* structures by Sha *et al.*[57] and Kersting *et al.* [58] However, due to a strong damping of the plasma oscillations excited by short optical pulses, only few-cycle THz signals have been observed.

Recently, Ryzhii et al [6] predicted that modulated infrared radiation can cause the resonant excitation of plasma oscillations in quantum well diode and transistor structures (see Fig. 15 and 16). This effect provides a new mechanism for the generation of tunable terahertz radiation using photomixing of infrared signals. They developed a device model for a Quantum Well Photo Mixer (QWPM) and calculated its high-frequency performance. It was shown that the proposed device can significantly surpass photomixers utilizing standard quantum well infrared photodetectors.

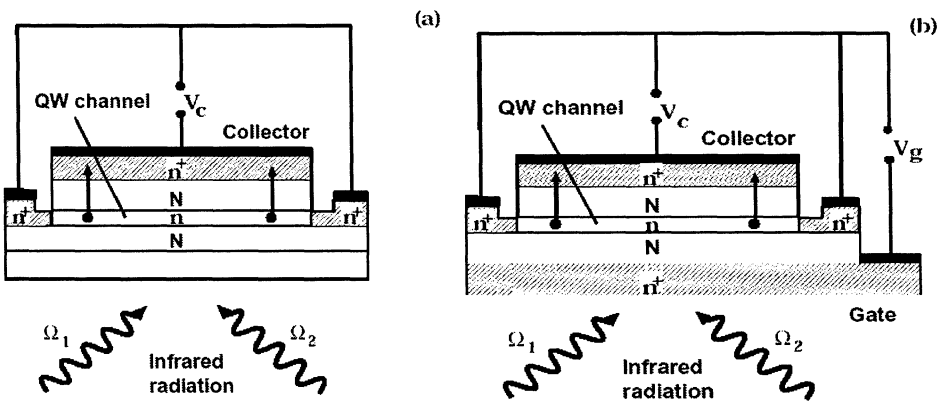

Fig. 15. Schematic view of diode-type (a) and transistor-type (b) QWPM structures without doping of the gate barrier and a band diagram of transistor-type QWPM (c). Arrows indicate electron trajectories (bound-to-continuum photoexcitation followed by transport over collector barrier). [6]

Ryzhii et al [6] also proposed a QWPM based on QW diode and transistor structures utilizing bound-to-continuum electron transitions, which can be used for photomixing, and evaluated the device operation using an analytical model. It was shown that the QWPM with high electron mobility in the QW channel can exhibit a resonant response to modulated infrared radiation when the modulation frequency is close to one of the plasma frequencies which can be in the THz range. High values of the responsivity in the THz range of signal frequencies indicated that the proposed QWPM and arrays of such devices can be used for efficient generation of THz radiation using photomixing of infrared signals.

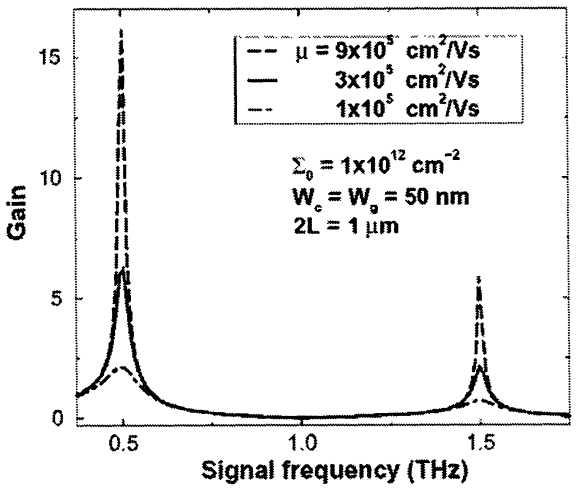

FIG. 16. Characteristic photoelectric gain vs signal frequency for QWPMs with different electron mobilities (different Q factors) in quantum well channel. [6]

Conclusions

Plasma wave excitation in submicron field effect transistors and related device structures should allow us to develop a new generation of solid-state terahertz tunable terahertz devices that will find numerous applications in industry, defense, and biotechnology. Recent experimental results demonstrated both resonant and non-resonant detection of terahertz radiation by plasma waves. These results are quite encouraging and indicate that proposed improved structures will be viable. New improved structures will use an enhancement of the plasma wave growth due to static or dynamic negative differential conductivity induced by the negative differential conductivity caused by the gate current.

Acknowledgment

This work has been partially supported by ARO (Project Monitor Dr. Dwight Woolard), by ONR (Project Monitor Dr. John Zolper), and by DARPA (Project Monitor, Dr. Edgar Martinez). We are grateful to Professor M. Dyakonov for useful comments and suggestions.

References

1. M. J. Rodwell, Editor, "High Speed Integrated Circuit Technology, Towards 100 GHz Logic", International Journal of High Speed Electronics and Systems, Vol. 11, No 1, March (2001)
2. M. I. Dyakonov and M. S. Shur, "Plasma Wave Electronics: Novel Terahertz Devices using Two Dimensional Electron Fluid", Special Issue on Future Directions in Device Science and Technologies, IEEE Transactions on Electron Devices, Vol. 43, No. 10, 1640-1646, October (1996)
3. M. Dyakonov and M. S. Shur, "Plasma Wave Electronics for Terahertz applications", pp. 187-207, in "Terahertz Sources and Systems", R. E. Miles, P. Harrison, and D. Lippens, Editors, NATO Science Series, II. Mathematics, Physics and Chemistry – Vol. 27, Kluwer Academic Publishers, Dordrecht/ Boston/ London, 2001
4 M. S. Shur and M. Dyakonov, Two-Dimensional Electrons in Field Effect Transistors, International Journal of High Speed Electronics and Systems, Vol. 9, No. 1, pp. 65-99, March (1998)
5. V. Ryzhii, I. Khmyrova, and M. S. Shur, "Resonant detection and frequency multiplication of terahertz radiation utilizing plasma waves in resonant-tunneling transistors", J. Appl. Phys. Vol. 88, No. 5, 2868-2871, 1 September (2000)
6. V. Ryzhii, I. Khmyrova, and M. S. Shur, "Terahertz photomixing in quantum well structures using resonant excitation of plasma oscillations", J. Appl. Phys. Vol. 91, 1875 (2002)
7. M. S. Shur and L. F. Eastman, "Ballistic Transport in Semiconductors at Low-Temperatures for Low Power High Speed Logic", IEEE Transactions Electron Devices, Vol. ED-26, No. 11, 1677-1683, November (1979)
8 G. Timp, J. Bude, K.K. Bourdelle, J. Garno, A. Ghetti, H. Gossmann, M. Green, G. Forsyth, Y. Kim, R. Kleiman, F. Klemens, A. Kornblit, C. Lochstampfor, W. Mansfield, S. Moccio, T. Sorsch, D.M. Tennant, W. Timp, R. Tung, The Ballistic Nano-Transistor, IEDM Tech. Digest, p.55-58 (1999)
9. H. Kawaura, T. Sakamoto, T. Baba, Y. Ochiai, Y., J. Fujita, J., and J. Sone, "Transistor Characteristics of 14-nm-Gate-Length EJ-MOSFETs", IEEE Trans. on Electron. Dev. **47**, 856-859 (2000).
10. A. A. Kastalsky and M. S. Shur, "Conductance of Small Semiconductor Devices", Solid State Comm. Vol. 39, No. 6, 715 (1981);
11. K. Lee and M. S. Shur, "Impedance of Thin Semiconductor Films", J. Appl. Phys. Vol. 54, No. 7, 4028-4034, July (1983)
12. M. Dyakonov and M. S. Shur, "Ballistic Transport in High Mobility Semiconductor", The Physics of Semiconductors ed. by M. Scheffler and R. Zimmermann (World Scientific, Singapore 1996), 145-148, (1996)
13. M. S. Shur, "Low Ballistic Mobility in Submicron High Electron Mobility Transistors", submitted for publication
14. M. S. Shur, "Ballistic Transport in Semiconductor with Collisions", IEEE Trans. Electron. Devices, Vol. ED-28, No. 10, 1120-1130, October (1981)
15. M. I. Dyakonov, and M. S. Shur, "Detection, Mixing, and Frequency Multiplication of Terahertz Radiation by Two Dimensional Electronic Fluid", IEEE Transactions on Electron Devices, 43, 380-387, (1996)

16 M. I. Dyakonov, and M. S. Shur, "Shallow Water Analogy for a Ballistic Field Effect Transistor", New Mechanism of Plasma Wave Generation by DC Current, Phys. Rev. Lett. 71, 2465-2468 (1993)
17. M. Dyakonov and M. S. Shur, "Plasma Wave Electronics for Terahertz applications", in "Terahertz Sources and Systems", R. E. Miles, P. Harrison, and D. Lippens, Editors, NATO Science Series, II. Mathematics, Physics and Chemistry – Vol. 27, 187-207, Kluwer Academic Publishers, Dordrecht/ Boston/ London (2001)
18. A. A. Ivanov and V. I. Ryzhii, "Collective relaxation of nonequilibrium photoelectrons in quantized magnetic fields", Zh. Eksper. Teor. Fiz. vol.63, no.4, 1514-1520, translated in Soviet Physics - JETP, vol.36, no.4, 803-806 (1972)
19. A. V. Chaplik, Zh. Eksp. Teor. Fiz. 62, 746 (Sov. Phys. JETP, 35, 395, (1972)
20. M. Nakayama, "Theory of surface waves coupled to surface carriers", J. Phys. Soc. Japan, 36, 393-398 (1974)
21. S. J. Allen, Jr., D. C. Tsui, and R. A. Logan, "Observation of the two-dimensional plasmon in silicon inversion layers", Phys. Rev. Lett. 38, 980 – 983, (1997)
22. D. C., Tsui, E. Gornik, and R. A. Logan, "Far infrared emission from plasma oscillations of Si inversion layers", Solid State Comm., 35, 875- 877, (1980)
23. P. J. Burke, I. B. Spielman, J. P. Eisenstein, L. N. Pfeiffer, and K. W. West, "High frequency conductivity of the high-mobility two-dimensional electron gas", Applied Phys. Lett. 76, 745-747, (2000)
24. J.-Q. Lü, M. S. Shur, J. L. Hesler, L. Sun, and R. Weikle, "A Resonant Terahertz Detector Utilizing a High Electron Mobility Transistor", IEDM'98 Technical Digest, San Francisco, CA, December (1998)
25. W. Knap, Y. Deng, S. Rumyantsev, J.-Q. Lu, M. S. Shur, C. A. Saylor , and L. C. Brunel, "Resonant detection of sub-Terahertz radiation by plasma waves in the submicron field effect transistor", accepted to Appl. Phys. Lett, accepted for publication
26. X. G. Peralta, S. J. Allen, N. E. Harff, M. C. Wanke, M. P. Lilly, J. A. Simmons, P. J. Burke, J. P. Eisenstein, "Terahertz Photoconductivity and Plasmon Modes in Double Quantum Well Field Effect Transistors", presented at Workshop on Frontiers of Electronics, St. Croix, VI (2002)
27. L. D. Landau and E. M. Lifshitz, *Fluid Mechanics* (Pergamon, New York, 1966)
28. V. L. Streeter and E. B. Wylie, *Fluid Mechanics*, ch. 7, (McGraw Hill, New York, 1985)
29. M. S. Shur, *Introduction to Electronic Devices* (John Wiley and Sons, New York, 1996, ISBN 0-471-10348-9)
30. M. Dyakonov and M. S. Shur, "Ballistic FET as Tunable Terahertz Oscillator", in Proceedings of 2d International Semiconductor Device Research Symposium, Charlottesville, VA, December, 741-744 (1993)
31 T. W. Crowe, R. J. Mattauch, R. M. Weikle, U. V. Bhapkar, Terahertz GaAs Devices and Circuits for Heterodyne Receivers, in *Compound Semiconductor Technology. The Age of Maturity*, M. S. Shur (ed.), World Scientific, pp. 209-246 (1996)
32. J.-Q. Lü and M.S. Shur, "Terahertz Detection by High Electron Mobility Transistor: Effect of Drain Current", Applied Phys. Lett., Vol. 78, No. 17, 2587-2588, April 23 (2001)
33. F. J. Crowne, J. Appl. Phys. Vol. 82, 1242-1254, (1997)

34. A. P. Dmitriev, V. Kachorovskii, and M. S. Shur, "Plasma Wave Instability in Field Effect Transistor", Applied Physics Letters, Volume 79, Issue 7, 922-924, August 13, (2001)
35. M. Cheremisin, M. Ph. D. Thesis, "Etude d'nstabilites un liquide bidimensionnel d'electrons dans un transistor a effect de champ", University of Montpellier (1999)
36 .V. Ryzhii, and M. S. Shur, "Plasma Instability and nonlinear terahertz oscillations in resonant-tunneling structures", Jpn. J. Appl. Phys. 40, 546-550 (2001)
37. S. Luryi and A. Zaslavsky, *Quantum Effect and Hot-Electron Devices*, in S. M. Sze (ed), Modern Semiconductor Devices, 253, Wiley, New York (1998)
38. V. Ryzhii, M. Willander, M. Ryzhii, I. Khmyrova, Heterostructure laser-transistors controlled by resonant-tunneling electron extraction", Semicond. Sci. Technol. 12, 431-438 (1997)
39. V. Ryzhii and M. S. Shur, "Terahertz plasma instability in two-dimensional tunneling-injection and barrier-injection transit-time structures", submitted to ICSNN2002
40. A. P. Dmitriev, A. S. Furman, V. Yu. Kachorovskii, G. G. Samsonidze, and Ge. G. Samsonidze, Phys. Rev. B, vol. 55, 10319-10325 (1997)
41. G. Samsonidze, S. Rudin, and M. S. Shur, "Large Signal Theory of Plasma Wave Electronics Terahertz Detectors", 1998 IEEE Sixth International Conference on Terahertz Electronics Proceedings, University of Leeds, IEEE Catalog Number: 98EX171, P. Harrison, Editor, 231-233 (1998)
42. Weikle, R. , Lu, J. , Shur, M. S., and Dyakonov, M. I., "Detection of Microwave Radiation by Electronic Fluid in High Electron mobility Transistors", Electronics Letters 32, 2148-2149, (1996)
43. Lü, J.-Q., Shur, M. S. , Hesler, J. L., Sun, L., and Weikle, R. "Terahertz Detector Utilizing Two-Dimensional Electronic Fluid", IEEE Electron Device Letters, 19, 373-375, (1998)
44. W. Knap, Y. Deng, S. Rumyantsev, J.-Q. Lu, M. S. Shur, C. A. Saylor , L. C. Brunel, Resonant detection of sub-Terahertz radiation by plasma waves in the submicron field effect transistor, accepted to Appl. Phys. Lett.
45 W. Knap, V. Kachorovskii, Y. Deng, S. Rumyantsev, J.-Q. Lu, R. Gaska, M. S. Shur, G. Simin, X. Hu and M. Asif Khan, C. A. Saylor, L. C. Brunel, Nonresonant Detection of Terahertz Radiation in Field Effect Transistors, J. Appl. Phys. vol. 91, No 10, May (2002)
46. J.-Q. Lü, M. S. Shur, R. Weikle, and M. I. Dyakonov, "Detection of Microwave Radiation by Electronic Fluid in AlGaN/GaN High Electron Mobility Transistors", in Proceedings of Sixteenth Biennial Conference on Advanced Concepts in High Speed Semiconductor Devices and Circuits, Ithaca, New York, Aug. 4-6, 211-217 (1997)
47. X.-C. Zhang, B. B. Hu, J. T Darrow, and D. H. Auston, Appl. Phys. Lett. 56, 1011 (1990)
48. E. G. Sun, G. A. Wagoner, and X.-C. Zhang, Appl. Phys. Lett. 67, 1656 (1995).
49. E. R. Brown, K. A. McIntosh, K. B. Nichols, and C. L. Dennis, Appl. Phys. Lett. 66, 285 (1995)
50. C. Ludwig and J. Kuhl, Appl. Phys. Lett. 69, 1194 (1996)
51. S. Verghese, K. A. McIntosh, and E. R. Brown, Appl. Phys. Lett. 71, 2743 (1997)

52. H. C. Liu, J. Li, E. R. Brown, K. A. McIntosh, K. B. Nichols, and M. J. Manfra, Appl. Phys. Lett. 67, 1594 (1995)
53. V. Ryzhii, I. Khmyrova, and M. Ryzhii, "Impact of transit-time and capture effects on high-frequency," IEEE Trans. Electron Devices 45, 293-298 (1998)
54. V. Ryzhii, "High-frequency performance of single quantum well infrared photodetectors at high power densities," IEEE Trans. Electron Dev. 45, 1797-1803 (1998).
55. M. Ryzhii and V. Ryzhii, "Monte Carlo analysis of ultra-fast electron transport in quantum well infrared photodetectors," Appl. Phys. Lett. 72, 842-844 (1998)
56. M. Ryzhii, V. Ryzhii, and M. Willander, "Monte Carlo modeling of electron velocity overshoot effect in quantum well infrared photodetectors", J. Appl. Phys. 84, 3403-3408 (1998)
57 W. Sha, A. Smirl, and W. Tseng, Phys. Rev. Lett. 74, 4273 (1995)
58. R. Kersting, K. Unterrainer, G. Strasser, H. F. Kauffmann, and E. Gornik, Phys. Rev. Lett. 79, 3038 (1997)